Journal of Molecular Graphics and Modelling 29 (2010) 206–213

Contents lists available at ScienceDirect

Journal of Molecular Graphics and Modelling

journal homepage: www.elsevier.com/locate/JMGM

Theoretical investigation of the interaction of glycerol with aluminum and magnesium phthalocyanines

V.H.C. Silva, L.T.F.M. Camargo, H.B. Napolitano, C.N. Pérez, A.J. Camargo*

Unidade Universitária de Ciências Exatas e Tecnológicas, Universidade Estadual de Goiás, P.O. Box 459, 75001-970, Anápolis, GO, Brazil

ARTICLE INFO

Article history:
Received 11 March 2010
Received in revised form 10 June 2010
Accepted 17 June 2010
Available online 25 June 2010

Keywords:
Glycerol
Glycerin
Metallophthalocyanine
Aluminum phthalocyanine
Magnesium phthalocyanine
B3LYP

ABSTRACT

Glycerol is a byproduct produced in great quantity by biodiesel industries in transesterification reactions. Finding new applications for glycerol is a current concern of many research groups around the world. This work focuses on a theoretical investigation, at the B3LYP/6-31G* level of theory, into the possibility of using aluminum phthalocyanine (AlPc) and magnesium phthalocyanine (MgPc) in the modelling of catalysts to convert glycerol into alcohol, which has wider industrial applicability. According to our calculations there are strong interactions between the O-terminus of glycerol and the central metal atom of AlPc and MgPc. By applying the Fukui function, HSAB theory and analysis of the frontier molecular orbital, it was possible to explain the way in which glycerol interacts with AlPc and MgPc. As a result of these interactions, there is a considerable change in both electronic and geometric parameters of glycerol, which can be used in designing new strategies to convert glycerol into alcohol.

1. Introduction

Biodiesel is an important alternative fuel for diesel engines, especially because of decreasing petroleum reserves and the need to seek more environmentally friendly fuels. It is produced from renewable biological sources such as vegetable oils and animal fats. Chemically, biodiesel consists of the simple alkyl esters of fatty acids and it is considered to contribute much less to global warming than fossil fuels [1–3]. Biodiesel is produced through the chemical reaction of a vegetable oil or animal fat with methanol or ethanol in the presence of an alkaline catalyst to produce fatty acid, esters, and glycerol. The process involving the reaction of a triglyceride such as vegetable oil with an alcohol is known as transesterification reaction. Glycerol is a byproduct of this reaction, and it creates a considerable problem for commercial biodiesel industries, since for every 90 m^3 of biodiesel produced by transesterification reaction about 10 m^3 of glycerol is generated [4,5]. What was once a valuable commodity now frequently entails high cost. Finding a solution to the glycerol byproduct problem has become a top priority for many biodiesel industries around the world [6,7]. The present work investigates, on theoretical grounds, the possibility of using aluminum and magnesium phthalocyanines as catalysts in the conversion of glycerol into alcohols, which have many industrial applications. In addition, the conversion of glycerol into alcohols makes the process of biodiesel purification easier. The alcohols produced can then be used in the transesterification reaction, reducing the production cost of biodiesel or even using it as a biofuel.

Phthalocyanines are macrocyclic compounds not found in nature that are able to coordinate hydrogen and metal cations in their centres, by coordinate bonds with the four isoindole nitrogen atoms. Most of the metals have been found capable of coordinating with the phthalocyanine macrocycle. Metallophthalocyanine complexes (MPc) are particularly attractive as potential catalysts for organic reactions because of their inexpensive and simple preparation on a large scale and their chemical and thermal stability [8–12]. Metallophthalocyanines are insoluble in common organic solvents, and they can easily be separated from the reaction mixture by filtration and reused without further treatment. Additionally, there is no pore size problem associated with their use. Among the many remarkable results obtained with phthalocyanines, their catalytic properties are of special interest, especially those of metallophthalocyanines (MPc). MPc's have been used extensively to catalyze a variety of organic reactions [13–21]. Aluminum and magnesium metals are an interesting choice for the phthalocyanine complex due to their small size and high charge density, which make strong electrostatic interaction possible and, in turn, a variation in the charge density of the ligands attached to them [22–25]. Furthermore, the catalytic properties of aluminum and magnesium phthalocyanines are not yet fully understood, especially for organic reactions [25–28].

The nature of the interactions between chemical reagents is better understood by carrying out calculations on the interaction

* Corresponding author. Tel.: +55 62 33281162; fax: +55 62 33281155.
E-mail address: ajc@ueg.br (A.J. Camargo).

1093-3263/$ – see front matter © 2010 Published by Elsevier Inc.
doi:10.1016/j.jmgm.2010.06.007

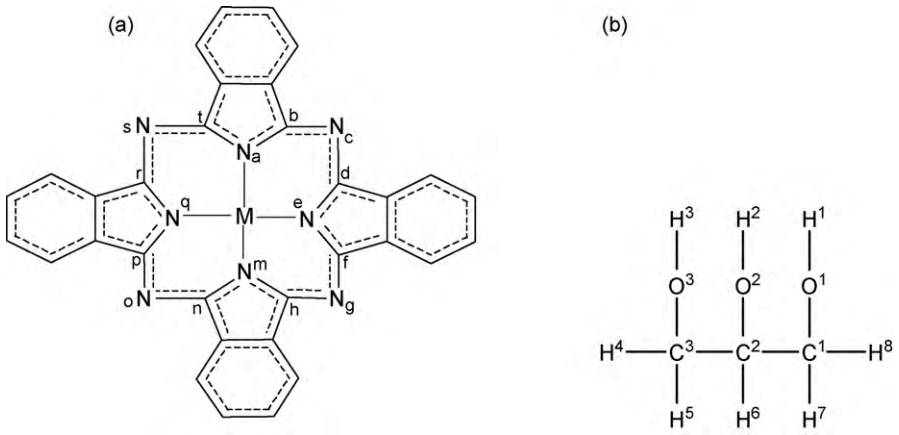

Fig. 1. Atomic numbering adopted in the calculation for (a) metallophthalocyanine and (b) glycerol.

energies and by global and local descriptors of electronic structure, such as chemical *hardness* (η), *softness* (S), and *Fukui functions* (f). These parameters have provided useful information about thermodynamic aspects of chemical reactions and reactivity sites [29–32]. The Hard–Soft Acid–Base (HSAB) principle utilizes the parameters' hardness and softness to state that "*hard acids* prefer to coordinate to *hard bases*, and *soft acids* to *soft bases*" [29,33]. The *Fukui function* is a local parameter responsible for identifying privileged sites of reactivity in the molecules and it states that the largest *Fukui function* value in the molecule is the preferable site for the reaction to take place.

In this paper, we describe the binding energies of glycerol bonded to aluminum phthalocyanine (AlPc) and magnesium phthalocyanine (AlPc), the population analysis, and the Fukui functions for the reagents. The Fukui functions were calculated in order to identify specific sites of glycerol, AlPc, and MgPc at which the interaction between two reagents is most likely to occur.

2. Computational procedure

The geometry and nomenclature used in the calculations for metallophthalocyanines and glycerol are shown in Fig. 1a and b, respectively. The calculations reported in this work were carried out using the Kohn–Sham density functional theory (DFT) with Beck three-parameters hybrid exchange-correlation functional, known as B3LYP [34–36], and the split-valence basis set 6-31G*, implemented in the Gaussian 03 program suite [37]. The local minima on the potential energy hypersurface were characterized by the computation of the vibrational frequencies at the same level of theory used in the geometry optimizations. The absence of vibrational modes with imaginary frequencies shows that the optimized molecular geometries are at a local minimum in the potential energy hypersurface. Since the binding energies include a basis set superposition error (BSSE) [38,39], due to the supermolecule approach, the full counterpoise method of Boys and Bernardi [40] was employed to estimate the BSSE, resulting in the corrected binding energy (ΔE) values. All the bond order indexes were obtained from natural population analysis (NPA) using the NBO 3.1 [41] program implemented in the Gaussian 03 program package. The atomic partial charges on the atoms were obtained from Merz–Singh–Kollman (MK) scheme [42,43] at B3LYP/6-31G* level of theory. In the Merz–Singh–Kollman scheme, atomic charges are fitted to reproduce the molecular electrostatic potential (MEP) at a number of points around the molecule. At first, the MEP is calculated at a number of grid points located on several layers around the molecule. The layers are constructed as an overlay of van der Waals spheres around each atom. The points located inside the van der Waals volume are neglected.

Since zero-point vibrational energy (ZPVE) contributions have a non-negligible effect on the stabilities of glycerol bonded to the metallophthalocyanines, we have evaluated these contributions using the B3LYP/6-31G* level of theory for glycerol complexed with AlPc and MgPc, respectively. The corrected binding energies for the complexes were calculated according to equation [44]

$$\Delta E = [E(\mathrm{GMPc}) + E(\mathrm{GMPc})_{\mathrm{ZPVE}}] - [E(\mathrm{MPc})_{\mathrm{BSSE}} + E(\mathrm{MPc})_{\mathrm{ZPVE}} + E(\mathrm{G})_{\mathrm{BSSE}} + E(\mathrm{G})_{\mathrm{ZPVE}}],$$

where ΔE represents the interaction energy, E is the calculated energy at B3LYP/6-31G* level of theory for each species, G represents the glycerol and M stands for Al or Mg, and Pc is the phthalocyanine. The general reaction for the complex formation can be written in a general way as G + MPc → GMPc, where the symbols have the same meaning as above. The hardness (η) and softness (S) were obtained using the equations $\eta = E(N_0 - 1) - 2EN_0 + E(N_0 + 1)$ and $S = 1/\eta$, where E stands for ground-state energy and N_0 is the number of electrons in the system's ground state. The Fukui functions (f) were calculated according to equations $f_x^+ \approx \rho_x^{\mathrm{HOMO}} = \sum_i |c_i|^2_{\mathrm{HOMO}}$, $f_x^- \approx \rho_x^{\mathrm{LUMO}} = \sum_i |c_i|^2_{\mathrm{LUMO}}$, and $f_x^0 \approx f_x^+ + f_x^-/2$, which is implemented in the MOCALC program [45,46]. These equations govern the nucleophilic, electrophilic, and radical attacks, respectively. In the Fukui function above, x stands for atom specification and c_i's are the coefficients for atom x in the frontier molecular orbital.

3. Results and discussion

3.1. Geometries of glycerol, $[AlPc]^0$, $[AlPc]^+$, $[MgPc]^0$, and $[MgPc]^+$

The structural parameters of glycerol fully optimized in gas phase at B3LYP/6-31G* level of theory are shown in Table 1 and Table 2. The results fit very well with those obtained by Raman et al. [47] at B3LYP/6-31+G* level of theory with an average absolute deviation less than 0.005 Å. The calculated bond lengths in this paper have an average absolute deviation from the experimental data [48] of about 0.017 Å (see Table 2).

In the formation of AlPc and MgPc complexes, phthalocyanine was considered as dianion (2−) and the Al and Mg cations were considered in their most stable oxidation state, *i.e.*, 3+ for Al and 2+ for Mg. As a result, we have the complexes $[AlPc]^+$ and $[MgPc]^0$ for aluminum and magnesium phthalocyanine, respectively. But we have also studied the reduced state for AlPc ($[AlPc]^0$) and the oxidized state for MgPc ($[MgPc]^+$). The first step in this investi-

Table 1
Theoretical and experimental bond lengths (in Å) and angle (in°) for aluminum and magnesium phthalocyanines in their reduced and oxidized states.

	$[AlPc]^0$	$[AlPc]^+$	$[(AlPc)Cl]^0$[a]	$[MgPc]^0$	$[MgPc]^+$	$[MgPc]^0$[b]
$M–N_a$	2.020	1.923	1.961	2.008	2.002	2.021
$M–N_e$	2.020	1.923	1.957	2.008	2.002	2.021
$M–N_m$	2.020	1.923	1.963	2.008	2.002	2.021
$M–N_q$	2.020	1.923	2.022	2.008	2.002	2.021
M-Plane	0.559	0.000	0.399	0.000	0.000	0.461
$N_a–C_b$	1.380	1.401	1.337	1.372	1.373	1.375
$C_b–N_c$	1.324	1.318	1.402	1.333	1.333	1.327
$N_c–C_d$	1.324	1.318	1.286	1.333	1.333	1.327
$C_d–N_e$	1.380	1.401	1.459	1.372	1.373	1.375
$N_e–C_f$	1.380	1.401	1.465	1.372	1.373	1.375
$C_f–N_g$	1.324	1.318	1.334	1.333	1.333	1.327
$N_g–C_h$	1.324	1.318	1.341	1.333	1.333	1.327
$C_h–N_m$	1.380	1.401	1.452	1.372	1.373	1.375
$N_m–C_n$	1.380	1.401	1.501	1.372	1.373	1.375
$C_n–N_o$	1.324	1.318	1.529	1.333	1.333	1.327
$N_o–C_p$	1.324	1.318	1.263	1.333	1.333	1.327
$C_p–N_q$	1.380	1.401	1.417	1.372	1.373	1.375
$N_q–C_r$	1.380	1.401	1.431	1.372	1.373	1.375
$C_r–N_s$	1.324	1.318	1.330	1.333	1.333	1.327
$N_s–C_t$	1.324	1.318	1.375	1.333	1.333	1.327
$C_t–N_a$	1.380	1.401	1.473	1.372	1.373	1.375
$N_a–M_e–N_m$	147.86	179.99	154.94	179.77	179.84	153.63
$N_e–M_e–N_q$	147.86	179.99	157.24	179.77	179.84	153.63

[a] X-ray values for $[AlPc(Cl)]^0$ from Ref. [49].
[b] X-ray values for $[MgPc]^0$ from Ref. [50].

gation was to perform a full optimization of these complexes in gas phase at the B3LYP/6-31G* level of approximation. The calculation results are shown in Table 1. The data analysis shows that the aluminum phthalocyanine in its oxidized state ($[AlPc]^+$) in gas phase has a planar geometrical structure with D_{4H} symmetry. In its reduced state ($[AlPc]^0$), the molecular geometry structure changes significantly. The main change is the projection of the Al atom out of molecular plane in about 0.56 Å and the symmetry change for C_{4V}. This value is 0.16 Å greater than the X-ray data [49] for chloro(phthalocyaninato)aluminum(III) $[(AlPc)Cl]^0$. The presence of the chloride ion and the intermolecular interactions in the solid state decrease the out-of-plane projection of Al atom. Furthermore, the observed disorder on $[(AlPc)Cl]^0$ crystal structure refined by Wynne [49] gave high overall refinement index values. The average absolute deviation of the calculated experimental values for the bond length is about 0.06 Å (see Table 1), which should indicate that the AlPc obtained experimentally is adsorbed with chloro and the AlPc obtained by us is theoretically free of chloride. For this reason some data are somewhat discrepant.

The calculated data also show an increase of 0.1 Å in the bond length Al–N in the reduced state, showing that this bonding is weaker in the reduced state than in the oxidized state. Except for a small decrease of 1.4° in the Al···N–C angle, the other geometrical parameters are not significantly changed with the reduction of AlPc.

The analysis of the frontier molecular orbitals helps to clarify this behaviour. In the oxidized state, AlPc is a complex with closed shell, *i.e.*, it presents all its electrons paired and multiplicity 1. The highest molecular orbital (HOMO) of $[AlPc]^+$ is a π bonding orbital located entirely on the phthalocyanine ring, and it does not have any contribution in the central region of AlPc where the Al atom is located (Fig. 1a). When the $[AlPc]^+$ complex is reduced by adding an extra electron, the complex becomes an open shell system with multiplicity 2. In this case, electrons α and β should be separated in the calculation. So, two HOMO orbitals are calculated: HOMO-α and HOMO-β. The HOMO-β does not contribute to the Al–N bonding. However, the HOMO-α orbital is localized in the molecular region where Al is bonded to phthalocyanine. This orbital has a strong σ^*

Table 2
Bond length (in Å) and dihedral angle (in°) for the glycerol in gas phase and the glycerol adsorbed by AlPc and MgPc in the reduced and oxidized state.

	Glycerol	Glycerol[a]	Exp[b]	$[G^\alpha AlPc]^0$	$[G^\alpha AlPc]^+$	$[G^\alpha MgPc]^0$	$[G^\alpha MgPc]^+$	$[G^\beta AlPc]^0$	$[G^\beta AlPc]^+$	$[G^\beta MgPc]^0$	$[G^\beta MgPc]^+$
Me–X[c]	–		–	1.959	1.938	2.096	2.060	1.980	1.950	2.104	2.091
$H^1–O^1$	0.978	0.968	–	0.992	0.994	0.982	0.987	0.968	0.969	0.971	0.969
$O^1–C^1$	1.426	1.432	1.401	1.449	1.458	1.442	1.444	1.432	1.433	1.432	1.433
$H^2–O^2$	0.976	0.973	–	0.981	0.977	0.970	0.969	0.988	0.994	0.981	0.985
$O^2–C^2$	1.429	1.425	1.435	1.427	1.430	1.422	1.417	1.460	1.469	1.445	1.459
$H^3–O^3$	0.973	0.968	–	0.971	0.969	0.968	0.969	0.968	0.969	0.971	0.970
$O^3–C^3$	1.433	1.438	1.437	1.428	1.421	1.435	1.438	1.422	1.416	1.413	1.413
$C^2–C^1$	1.537	1.532	1.509	1.541	1.532	1.537	1.532	1.528	1.533	1.529	1.529
$C^3–C^2$	1.533	1.526	1.509	1.542	1.531	1.528	1.534	1.523	1.524	1.532	1.527
$H^8–C^1$	1.094	1.098	–	1.093	1.093	1.097	1.097	1.099	1.093	1.097	1.096
$H^7–C^1$	1.100	1.099	–	1.092	1.091	1.092	1.091	1.094	1.098	1.092	1.097
$H^6–C^2$	1.100	1.096	–	1.098	1.098	1.099	1.100	1.094	1.093	1.101	1.097
$H^5–C^3$	1.095	1.097	–	1.091	1.100	1.099	1.098	1.101	1.098	1.097	1.100
$H^4–C^3$	1.100	1.099	–	1.098	1.099	1.097	1.098	1.095	1.101	1.098	1.095
D1	−57.29	–	66.56	35.81	49.44	−174.90	−176.52	173.35	−174.90	42.76	62.56
D2	47.02	–	−59.57	36.60	40.96	−173.81	−176.67	45.92	−40.08	62.422	43.74

[a] From Ref. [47]
[b] From Ref. [48]
[c] Me = Al or Mg and X = O^1 or O^2 of glycerol (see Fig. 1b), G stands for glycerol, D1 and D2 stand for $O3–C^3–C^2–O^2$ and $O^2–C^2–C^1–O^1$ dihedral angles, respectively.

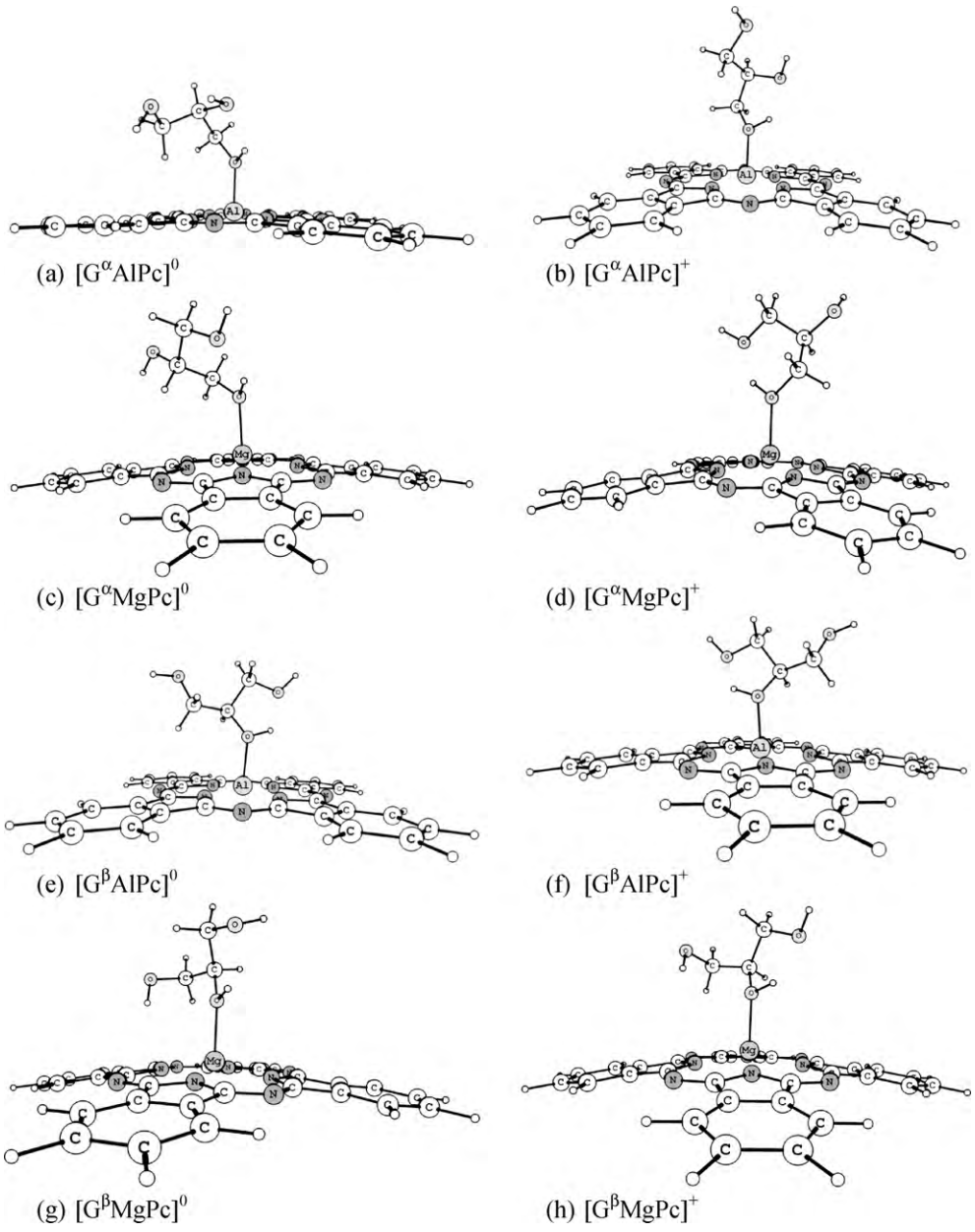

Fig. 2. Optimized structures using the B3LYP/6-31G* level of theory for glycerol adsorbed by AlPc and MgPc in the reduced and oxidized states.

(antibonding) character between Al and nitrogen to the Al atoms. It turns out that placing an electron in this orbital decreases the bond order of the Al–N bond from 0.40 to 0.29, representing a decrease of 27.5% in this bonding strength. These results are in close agreement with the projection of the Al atom out of the molecular plane in the reduced state ([AlPc]^{0}).

The symmetry found for [MgPc]$^{+}$ and [MgPc]^{0} complexes in gas phase at B3LYP/6-31G* level of theory is D_{4H} for both. It means that both structures are planar and the distance Mg–N is very close to Al–N distance of the [AlPc]^{0} complex (see Table 1). Table 1 also shows the geometrical parameters for MgPc, which do not change significantly when [MgPc]^{0} is oxidized. The average absolute bond length deviation between the calculated and the experimental values [50] for [MgPc]^{0} is 0.0062 Å. However, our calculation in gas phase predicts a planar structure for MgPc in both oxidation states, and the X-ray data show a projection of the Mg atom out of the molecular plane of 0.461 Å. Nevertheless, in the solid state, two magnesium phthalocyanine monomers are close enough to allow the Mg atom to make a weak bond with azamethine nitrogen, forming a dimer [50].

Frontier molecular orbital theory also explains why geometrical parameters for MgPc do not change when MgPc is oxidized. The HOMO orbital for [MgPc]^{0} is located entirely on the phthalocyanine macrocycle ring; it is doubly occupied and has a π nonbonding character. Removing an electron from this orbital does not affect the nature of the bonding between the atoms of MgPc.

3.2. The interaction of glycerol with AlPc and MgPc

Initially, the interaction of hydrogen from the glycerol hydroxyl group with the Al and Mg of AlPc and MgPc, respectively, was investigated. The calculation results carried out at B3LYP/6-31G* level of theory show that no hydrogen from glycerol can interact with Al or Mg. All attempts to optimize structures with hydrogen from glycerol bonded to Al or Mg led to molecular structures in which it is oxygen that bonds to the metallic atom. This result was expected,

Table 3
The calculated bond energies at the B3LYP/6-31G* level of theory including the BSSE and ZPVE corrections.

Reaction of complex formation	Binding energy in kcal/mol
$G + [AlPc]^0 \rightarrow [G\alpha AlPc]^0$	−38.95
$G + [AlPc]^+ \rightarrow [G\alpha AlPc]^+$	−45.53
$G + [MgPc]^0 \rightarrow [G\alpha MgPc]^0$	−27.08
$G + [MgPc]^+ \rightarrow [G^{\alpha}MgPc]^+$	−36.08
$G + [AlPc]^0 \rightarrow [G^{\beta}AlPc]^0$	−34.79
$G + [AlPc]^+ \rightarrow [G^{\beta}AlPc]^+$	−44.97
$G + [MgPc]^0 \rightarrow [G^{\beta}MgPc]^0$	−23.92
$G + [MgPc]^+ \rightarrow [G^{\beta}MgPc]^+$	−29.93

G stands for glycerol.

because the metallic atoms in the $[AlPc]^0$, $[AlPc]^+$, $[MgPc]^0$, and $[MgPc]^+$ complexes are electrophilic sites and hydrogen from glycerol is electron-deficient.

The geometrical parameters fully optimized for the glycerol adsorbed by AlPc and MgPc are shown in Table 2. In this work, G^{α} stands for glycerol bonded to AlPc or MgPc by O^1 atom, and G^{β} stands for glycerol bonded to AlPc or MgPc by O^2 atom. Table 2 shows a strong coordination of the oxygen from glycerol with the metals of AlPc and MgPc. This bonding is shorter for AlPc than MgPc, indicating that the glycerol is more strongly bonded to AlPc than to MgPc (see Fig. 2). The calculated values of the O–metal bond length are 1.959 Å, 1.938 Å, 2.096 Å, 2.060 Å, 1.980 Å, 1.950 Å, 2.104 Å, and 2.091 Å for $[G^{\alpha}AlPc]^0$, $[G^{\alpha}AlPc]^+$, $[G^{\alpha}MgPc]^0$, $[G^{\alpha}MgPc]^+$, $[G^{\beta}AlPc]^0$, $[G^{\beta}AlPc]^+$, $[G^{\beta}MgPc]^0$, and $[G^{\beta}MgPc]^+$ complexes, respectively. These results also show clearly that the oxidation state of the metallophthalocyanines is important in the G–metal bond formation, especially for AlPc complex. The bond energies obtained at B3LYP/6-31G* level and corrected by ZPVE and BSSE are shown in Table 3. The analysis of these data shows that the binding energies are favourable to the formation of all complexes under study. However, $[G^{\alpha}AlPc]^+$ and $[G^{\beta}AlPc]^+$ have the strongest interaction energies with −45.53 kcal/mol and −44.97 kcal/mol, respectively. The lowest binding energy (−23.92 kcal/mol) is calculated for $[G^{\beta}MgPc]^0$ complex, which has also the longest bond length (2.104 Å). The H^1–O^1 bond length increases about 1.43% in the $[G^{\alpha}AlPc]^0$ and $[G^{\alpha}AlPc]^+$ complexes when compared to the free glycerol. The increase in the H^1–O^1 bond length in both $[G^{\alpha}MgPc]^0$ and $[G^{\alpha}MgPc]^+$ is only about 0.9%. Similar values are found for H^2–O^2 bond length when the glycerol is bonded to Al and Mg by the O^2 atom. The O^1–C^1 bond length is also increased by about 2.24% when the glycerol is bonded to Al in the $[G^{\alpha}AlPc]^0$ and $[G^{\alpha}AlPc]^+$ complexes, and about 1.26% when the glycerol is bonded to Mg in the $[G^{\alpha}MgPc]^0$ and $[G^{\alpha}MgPc]^+$ complexes. When the O^2 atom is bonded to the Al atom, the O^2–C^2 bond length is increased by 2.17% for $[G^{\beta}AlPc]^0$ and 2.8% for $[G^{\beta}AlPc]^+$, when compared to the free glycerol. For $[G^{\beta}MgPc]^0$ and $[G^{\beta}MgPc]^+$, the increase in the O^2–C^2 bond length of glycerol is smaller than for AlPc, *i.e.*, 1.12% and 2.1%, respectively.

The bond order indices give us an idea of the electronic density between adjacent atoms. Increasing the bond order leads to an increase in the bond strength between adjacent atoms. Table 4 shows a change in the calculated bond orders for C–OH and O–H bonding of glycerol when it is bonded to Al and Mg. The bond order O^1–H^1 decreases by about 14% and 11% for glycerol bonded to AlPc and MgPc, respectively. This result implies a considerable weakening of the O^1–H^1 bond as a result of the adsorption of glycerol by AlPc and MgPc. A similar decrease is observed for the O^2–H^2 bond in the $G^{\beta}AlPc$ and $G^{\beta}MgPc$ complexes, *i.e.*, about 15% and 9%, respectively. The C^1–O^1 bond order also decreases by about 9% and 5% for the $G^{\alpha}AlPc$ and $G^{\alpha}AlPc$ complexes, respectively. When the glycerol is adsorbed by the O^2 atom, the effect on the C^2–O^2 bond order is less pronounced: about 10% and 8% for $G^{\beta}AlPc$ and $G^{\beta}MgPc$, respectively.

Table 5 shows the partial atomic charges (in *e* units) obtained from Merz–Singh–Kollman population analysis at B3LYP/6-31G* level of approximation, for glycerol in gas phase and adsorbed by AlPc and MgPc. Atomic partial charges are generally used by chemists for a qualitative understanding of structure and reactivity of molecules. In this regard, the atomic partial charges are important when proposing chemical reaction sites. The calculation results show the aluminum atom presenting a high positive charge, with values varying from 1.38*e* up to 1.48*e*. The highest positive value is observed for $[G^{\beta}AlPc]^0$, and the lowest positive value is observed for $[G^{\alpha}AlPc]^0$. A similar result is observed for the Mg atom by means of charge ranging from 0.98*e* to 1.01*e*.

Table 5 shows a great variation in atomic partial charges on H^1, H^2, O^1, and O^2 atoms of glycerol due to the complexation of glycerol with AlPc and MgPc. For H^1 atom, the charge value increases in the $[G^{\alpha}MgPc]^0$ and $[G^{\alpha}MgPc]^+$ complexes, and decreases in the $[G^{\alpha}AlPc]^0$ and $[G^{\alpha}AlPc]^+$ complexes when compared to the free glycerol. For the H^2 atom, the atomic partial charge increases in the $[G^{\beta}AlPc]^0$ and $[G^{\beta}AlPc]^+$ complexes, and decreases in the $[G^{\beta}MgPc]^0$ and $[G^{\beta}MgPc]^+$ complexes. The charge on O^1 increases its negative value in the $[G^{\beta}MgPc]^0$ and $[G^{\beta}MgPc]^+$, and decreases in the $[G^{\beta}AlPc]^0$ and $[G^{\beta}AlPc]^+$ complexes. The partial charge on the O^2 atom has its negative value greatly enhanced in the $[G^{\beta}AlPc]^0$ and $[G^{\beta}AlPc]^+$ complexes, making it more susceptible to nucleophilic attack. The atomic partial charge on O^2 in the $[G^{\beta}AlPc]^0$ and $[G^{\beta}AlPc]^+$ complexes does not change significantly (see Table 5). In short, the interaction of glycerol by AlPc or MgPc changes the electronic and geometric structure of glycerol, especially in the OH group, when the oxygen of the hydroxyl group is bonded to the Al or Mg of AlPc and MgPc complexes.

Table 4
Bond order for glycerol alone and glycerol adsorbed by AlPc and MgPc.

	Glycerol	$[G^{\alpha}AlPc]^0$	$[G^{\alpha}ALPC]^+$	$[G^{\alpha}MGPC]^0$	$[G^{\alpha}MGPC]^+$	$[G^{\beta}AlPc]^0$	$[G^{\beta}ALPC]^+$	$[G^{\beta}MGPC]^0$	$[G^{\beta}MGPC]^+$
Me–X[a]	–	0.230	0.240	0.086	0.094	0.222	0.239	0.083	0.091
H^{φ}–O^{α}	0.710	0.611	0.610	0.649	0.629	0.737	0.725	0.751	0.732
O^{α}–C^{γ}	0.939	0.860	0.847	0.889	0.882	0.917	0.913	0.923	0.917
H^{ξ}–O^{β}	0.719	0.676	0.688	0.747	0.745	0.631	0.611	0.664	0.651
O^{β}–C^{λ}	0.927	0.926	0.918	0.931	0.938	0.842	0.833	0.866	0.854
H^{δ}–O^{π}	0.739	0.727	0.735	0.736	0.729	0.748	0.741	0.734	0.750
O^{π}–C^{σ}	0.923	0.928	0.933	0.906	0.901	0.936	0.944	0.955	0.954
C^{λ}–C^{γ}	0.992	0.992	0.998	0.987	0.991	0.997	0.996	0.993	0.997
C^{σ}–C^{λ}	0.989	0.986	0.993	0.990	0.987	0.994	0.994	0.990	0.996
H^{η}–C^{γ}	0.917	0.912	0.910	0.917	0.914	0.920	0.900	0.919	0.908
H^{κ}–C^{γ}	0.919	0.914	0.912	0.915	0.913	0.903	0.918	0.900	0.909
H^{τ}–C^{λ}	0.894	0.895	0.885	0.897	0.898	0.890	0.892	0.900	0.896
H^{θ}–C^{σ}	0.917	0.920	0.917	0.916	0.917	0.913	0.914	0.908	0.903
H^{ρ}–C^{σ}	0.917	0.912	0.909	0.919	0.917	0.911	0.913	0.911	0.913

[a] Me = Al or Mg and X = O^1 or O^2 of glycerol molecule (see Fig. 1b for the atomic numbering adopted).

Table 5
Partial atomic charges (in *e* units)[a] obtained from Merz–Singh–Kollman population analysis at B3LYP/6-31G[a] level of theory for glycerol alone and adsorbed by AlPc and MgPc.

	Glycerol	$[G^{\alpha}AlPc]^0$	$[G^{\alpha}AlPc]^+$	$[G^{\alpha}MgPc]^0$	$[G^{\alpha}MgPc]^+$	$[G^{\beta}AlPc]^0$	$[G^{\beta}AlPc]^+$	$[G^{\beta}MgPc]^0$	$[G^{\beta}MgPc]^+$
Me[b]	–	1.385	1.455	0.997	0.970	1.482	1.429	0.938	1.011
H^1	0.388	0.323	0.366	0.426	0.411	0.449	0.465	0.408	0.368
H^2	0.364	0.379	0.426	0.405	0.420	0.416	0.429	0.377	0.375
H^3	0.365	0.375	0.448	0.443	0.447	0.474	0.471	0.371	0.430
H^4	0.049	−0.076	0.013	0.033	0.022	0.054	0.040	−0.006	0.091
H^5	0.058	−0.010	0.040	0.038	0.024	0.075	0.020	0.047	0.002
H^6	0.018	0.004	0.048	0.032	0.036	0.032	−0.024	0.020	0.070
H^7	0.037	0.025	0.120	0.003	0.057	0.063	0.049	0.062	0.020
H^8	0.084	0.092	0.153	0.041	0.077	0.033	0.091	−0.008	0.012
O^1	−0.570	−0.463	−0.480	−0.640	−0.636	−0.666	−0.663	−0.622	−0.632
O^2	−0.555	−0.562	−0.595	−0.630	−0.637	−0.757	−0.764	−0.543	−0.533
O^3	−0.553	−0.604	−0.642	−0.685	−0.663	−0.685	−0.691	−0.589	−0.535
C^1	0.057	0.052	0.208	0.229	0.149	0.101	0.060	0.274	0.136
C^2	0.164	0.270	0.352	0.183	0.235	0.662	0.593	0.066	0.028
C^3	0.094	0.302	0.137	0.204	0.193	−0.068	0.081	0.215	0.280
Total charge glycerol	0.000	0.107	0.594	0.082	0.135	0.183	0.157	0.072	0.112

[a] *e* = charge of one electron.
[b] Me = Al or Mg.

Table 6
Global hardness (η) and softness (S), and Fukui function f^0 calculated at B3LYP/6-31G* level of theory for the reactants glycerol, aluminum and magnesium phthalocyanines.

	η (eV)	S (eV)	f^0										
			C^3	H^2	H^3	O^1	O^2	O^3	C_b	N_a	N_c	Al	Mg
Glycerol	13.177	0.076	0.179	0.137	0.342	0.275	0.318	0.595	–	–	–	–	–
$[AlPc]^0$	3.694	0.271	–	–	–	–	–	–	0.030	0.031	0.007	0.401	–
$[AlPc]^+$	4.161	0.240	–	–	–	–	–	–	0.033	0.009	0.032	0.000	–
$[MgPc]^0$	4.403	0.227	–	–	–	–	–	–	0.034	0.025	0.023	–	0.000
$[MgPc]^+$	3.236	0.309	–	–	–	–	–	–	0.028	0.017	0.000	–	0.000

Table 7
Fukui functions f^+ and f^- calculated at B3LYP/6-31G* level of theory for the reagents glycerol and metallophthalocyanines.

	f^-		f^+	f^-		f^-			f^+		
	N_a	N_c	C_b	Al	Mg	O^1	O^2	O^3	C^3	H^2	H^3
Glycerol	–	–	–	–	–	0.113	0.233	0.180	0.078	0.002	0.003
$[AlPc]^0$	0.000	0.000	0.005	0.801	–	–	–	–	–	–	–
$[AlPc]^+$	0.000	0.000	0.013	0.000	–	–	–	–	–	–	–
$[MgPc]^0$	0.000	0.000	0.012	–	0.000	–	–	–	–	–	–
$[MgPc]^+$	0.034	0.000	0.057	–	0.000	–	–	–	–	–	–

3.3. Reactivity descriptors

From the results mentioned before, it is found that glycerol may complex with $[AlPc]^0$, $[AlPc]^+$, $[MgPc]^0$, and $[MgPc]^+$, forming the complexes $[GAlPc]^0$, $[GAlPc]^+$, $[GMgPc]^0$, and $[GMgPc]^+$, which, in terms of energy, are more stable than the reactants, as can be seen in Table 3. In order to seek a possible explanation for these complexation phenomena we have also calculated the Fukui functions and applied the theory of hard-and-soft acid–base (HSAB) in the reactants. The statement that "*soft likes soft*" and "*hard likes hard*", together with the idea that the larger the value of the Fukui function, the greater the reactivity, also provides a very useful approach to explain the chemical reactivity of many chemical systems [51–57]. The determination of the specific sites at which the interaction between two chemical species takes place is very important to elucidate the path and the products of a given reaction. As stated by Gázquez et al. [58] the largest value of the Fukui function is, in general, associated with the most reactive site. In this work, we are especially interested in describing the interaction of glycerol with Al of $[AlPc]^0$ and $[AlPc]^+$ and Mg of $[MgPc]^0$ and $[MgPc]^+$. According to the calculated data shown in Tables 6 and 7, the largest Fukui function ($f^0 = 0.596$) for glycerol is found to be at the O-terminus and, in turn, this site governs a radical interaction. For the metallophthalocyanine complexes, the largest calculated Fukui function ($f^+ = 0.801$) is at the Al atom of the $[AlPc]^0$ complex. The Fukui functions for Al and Mg for the other complexes ($[AlPc]^+$, $[MgPc]^0$, and $[MgPc]^+$) are zero. This result shows that the interaction of glycerol with $[AlPc]^0$ is through bond formation. Table 6 also shows that glycerol can be considered as hard base and the aluminum and magnesium phthalocyanines can be considered as hard acid. Hard base–hard acid interactions are charge controlled and depend mainly on the ionic interaction of the reagents. Therefore, by applying the global HSAB theory, the interaction between glycerol and $[GAlPc]^+$, $[GMgPc]^0$, and $[GMgPc]^+$ can be explained as being essentially an electrostatic interaction.

4. Conclusions

The calculation results at the B3LYP/6-31G* level showed that the $[AlPc]^+$ complex has D_{4H} molecular symmetry (planar structure), while the symmetry found for the $[AlPc]^0$ complex was C_{4V}, with the Al atom out of the molecular plane by about 0.6 Å. This change in the geometrical structure can be explained by analysing the HOMO orbital. The HOMO of $[AlPc]^0$ is centred on the Al atom and it presents an antibonding character, which makes the Al–N bonding weak and, in turn, takes the Al atom out of the molecu-

lar plane. The symmetry found for $[MgPc]^0$ and $[MgPc]^+$ was D_{4H} (planar structure), *i.e.*, the geometry of MgPc is not affected by oxidation. The interaction of glycerol with AlPc and MgPc is stronger for AlPc than for MgPc, and the oxidation state of the complexes affects the strength of the interaction. In addition, the electronic and geometrical structures of glycerol change considerably after complexation, especially for the O-terminus of glycerol bonded to Al or Mg. The main observed changes are an increase in the bonding length of C_1–O_1, O_1–H_1, C_2–O_2, O_2–H_2, and a decrease in the bond orders of the chemical bonds O_1–H_1 and O_2–H_2 by about 11% on average. For glycerol the largest Fukui function ($f^0 = 0.596$) is on O-terminus, showing that this site is the most favourable for the reaction to take place, and the largest Fukui function ($f^+ = 0.801$) for the reactant $[AlPc]^0$ is on the Al atom, showing that this site is undergoing nucleophilic attack. By applying the global HSAB theory, the interaction between glycerol and $[GAlPc]^+$, $[GMgPc]^0$, and $[GMgPc]^+$ can be explained as being essentially an electrostatic interaction. These results show that AlPc and MgPc can be used in designing the path reaction to convert glycerol into alcohol.

Acknowledgements

The authors would like to acknowledge the Pró-Reitoria de Pesquisa e Pós-Graduação (PrP) of the Universidade Estadual de Goiás (UEG) for financial support for this research. H.B. Napolitano is grateful for support from Coordenação de Aperfeiçoamento de Pessoal de Nível Superior, Brazil (process 2036-09-6).

References

[1] A. Demirbas, Progress and recent trends in biofuels, Prog. Energy Combust. 33 (2007) 1–18.
[2] J.V. Gerpen, Biodiesel processing and production, Fuel Process. Technol. 86 (2005) 1097–1107.
[3] F. Ma, M.A. Hanna, Biodiesel production: a review, Bioresour. Technol. 70 (1999) 1–15.
[4] C.J.A. Mota, C.X.A. Silva, V.L.C. Gonçalves, Gliceroquímica: novos produtos e processos a partir da glicerina de produção de biodiesel, Quím. Nova 32 (2009) 639–648.
[5] V.L.C. Gonçalves, B.P. Pinto, J.C. Silva, C.J.A. Mota, Acetylation of glycerol catalyzed by different solid acids, Catal. Today 133 (2008) 673–677.
[6] L. Bournay, D. Casanave, B. Delfort, G. Hillion, J.A. Chodorge, New heterogeneous process for biodiesel production: a way to improve the quality and the value of the crude glycerin produced by biodiesel plants, Catal. Today 106 (2005) 190–192.
[7] A. Wolfson, G. Litvak, C. Dlugy, Y. Shotland, D. Tavor, Employing crude glycerol from biodiesel production as an alternative green reaction medium, Ind. Crops Prod. 30 (2009) 78–81.
[8] A.W. Snow, W.R. Barger, in: C.C. Leznoff, A.B.P. Lever (Eds.), Phthalocyanines Properties and Applications, VCH Publishers, New York, 1989, p. 341.
[9] V.I. Iliev, A.I. Ileva, L.D. Dimitrov, Catalytic oxidation of 2-mercaptoethanol by cobalt(II)–phthalocyanine complexes intercalated in layered double hydroxides, Appl. Catal. A: Gen. 126 (1995) 333–340.
[10] V.H.C. Silva, A.J. Camargo, H.B. Napolitano, A.E. Oliveira, Estudo químico quântico da adsorção dos gases O_2 e H_2 sobre a ftalocianina de alumínio, Rev. Process. Quím. 2 (2008) 23–30.
[11] W. Galezowski, J. Kuta, P.M. Kozlowski, DFT study of Co–C bond cleavage in the neutral and one-electron-reduced, J. Phys. Chem. B. 112 (2008) 3177–3183.
[12] D. Rutkowska-Zbik, M. Witko, From activation of dioxygen to formation of high-valent oxo species: ab initio DFT studies, J. Mol. Catal. A: Chem. 275 (2007) 113–120.
[13] B. Meunier, A. Sorokin, Oxidation of pollutants catalyzed by metallophthalocyanines, Acc. Chem. Res. 30 (1997) 470–476.
[14] A. Sorokin, S. De Suzzoni-Dezard, D. Poullain, J.P. Noel, B. Meunier, CO_2 as the ultimate degradation product in the H_2O_2 oxidation of 2,4,6-trichlorophenol catalyzed by iron tetrasulfophthalocyanine, J. Am. Chem. Soc. 118 (1996) 7410–7411.
[15] A. Hadasch, A. Sorokin, A. Rabion, L. Fraisse, B. Meunier, Oxidation of 2,4,6-trichlorophenol (TCP) catalyzed by iron tetrasulfophthalocyanine (FePcS) supported on a cationic ion-exchange resin, Bull. Soc. Chim. Fr. 134 (1997) 1025–1032.
[16] A. Sorokin, B. Meunier, Efficient H_2O_2 oxidation of chlorinated phenols catalysed by supported iron phthalocyanines, J. Chem. Soc. Chem. Commun. (1994) 1799–1800.
[17] A. Sorokin, J.L. Seris, B. Meunier, Efficient oxidative dechlorination and aromatic ring cleavage of chlorinated phenols catalyzed by iron sulfophthalocyanine, Science 268 (1995) 1163–1166.
[18] K. Kasuga, K. Mori, T. Sugimori, M. Handa, Kinetic study on the oxidation of trichlorophenol using hydrogen peroxide and an iron(III) complex of tetrasulfonatophthalocyanine catalyst, Bull. Chem. Soc. Jpn. 73 (2000) 939–940.
[19] N. Grootboom, T. Nyokong, Iron perchlorophthalocyanine and tetrasulfophthalocyanine catalyzed oxidation of cyclohexane using hydrogen peroxide, chloroperoxybenzoic acid and tert-butylhydroperoxide as oxidants, J. Mol. Catal. 179 (2002) 113–123.
[20] Y. Huang, G.X. Xu, Y.R. Peng, et al., Study on the interaction of tetra-sulfonated phathalocyanine cobalt with bovine serum albumin, Spectrosc. Spect. Anal. 28 (2008) 407–411.
[21] S.L. Jain, J.K. Joseph, S. Singhal, B. Sain, Metallophthalocyanines (MPcs) as efficient heterogeneous catalysts for Biginelli condensation: application and comparison in catalytic activity of different MPcs for one pot synthesis of 3,4-dihydropyrimidin-2-(1H)-ones, J. Mol. Catal. A: Chem. 268 (2007) 134–138.
[22] C.A.T. Laia, S.M.B. Costa, L.F.V. Ferreira, Electron-transfer mechanism of the triplet state quenching of aluminum tetrasulfonated phthalocyanine by cytochrome c, Biophys. Chem. 122 (2006) 143–155.
[23] M. Pavlov, P.E.M. Siegbahn, M. Sandström, Hydration of beryllium, magnesium, calcium, and zinc ions using density functional theory, J. Phys. Chem. A 102 (1998) 219–228.
[24] I.G. Hill, J. Schwartz, A. Kahn, Metal-dependent charge transfer and chemical interaction at interfaces between 3,4,9,10-perylenetetracarboxylic bisimidazole and gold, silver and magnesium, Org. Electron. 1 (2000) 5–13.
[25] G. Rajagopal, S.S. Kim, J.M. Kwak, Aluminum phthalocyanine: an active and simple catalyst for cyanosilylation of ketones, Bull. Korean Chem. Soc. 27 (2006) 1907–1909.
[26] J. Janczak, M. Sledz, R. Kubiak, Catalytic trimerization of 2- and 4-cyanopyridine isomers to the triazine derivatives in presence of magnesium phthalocyanine, J. Mol. Struct. 659 (2003) 71–79.
[27] D. Ji, X. Lu, R. He, Syntheses of cyclic carbonates from carbon dioxide and epoxides with metal phthalocyanines as catalyst, Appl. Catal. A: Gen. 203 (2000) 329–333.
[28] X. Lu, H. Wang, R. He, Aluminum phthalocyanine complex covalently bonded to MCM-41 silica as heterogeneous catalyst for the synthesis of cyclic carbonates, J. Mol. Catal. A: Chem. 186 (2002) 33–42.
[29] R.G. Pearson, Hard and soft acids and bases, J. Am. Chem. Soc. 85 (1963) 3533–3539.
[30] R.G. Parr, R.G. Pearson, Absolute hardness: companion parameter to absolute electronegativity, J. Am. Chem. Soc. 105 (1983) 7512–7516.
[31] (a) R.G. Parr, W. Yang, Density functional approach to the frontier-electron theory of chemical reactivity, J. Am. Chem. Soc. 106 (1984) 4049–4950;
(b) W. Yang, R.G. Parr, Hardness, softness, and the Fukui function in the electronic theory of metals and catalysis, Proc. Natl. Acad. Sci. U.S.A. 82 (1985) 6723–6726.
[32] H. Chermette, Chemical reactivity indexes in density functional theory, J. Comput. Chem. 20 (1999) 129–154.
[33] P.K. Chattaraj, H. Lee, R.G. Parr, HSAB principle, J. Am. Chem. Soc. 113 (1991) 1855–1857.
[34] A.D. Becke, Density-functional thermochemistry. III. The role of exact exchange, J. Chem. Phys. 98 (1993) 5648–5652.
[35] C. Lee, W. Yang, R.G. Parr, Development of the Colle–Salvetti correlation-energy formula into a functional of the electron density, Phys. Rev. B 37 (1988) 785–789.
[36] B. Miehlich, A. Savin, H. Stoll, H. Preuss, Results obtained with the correlation energy density functionals of becke and Lee, Yang and Parr, Chem. Phys. Lett. 157 (1989) 200–206.
[37] M.J. Frisch, et al., Gaussian 03, Revision C.02, Gaussian, Inc., Wallingford, CT, 2004.
[38] N.R. Kestner, He–He interaction in the SCF-MO approximation, J. Chem. Phys. 48 (1968) 252–257.
[39] P. Salvador, S. Simon, M. Duran, J.J. Dannenberg, C–H. . .O–H-bonded complexes: how does basis set superposition error change their potential-energy surfaces? J. Chem. Phys. 113 (2000) 5666–5673.
[40] S.F. Boys, F. Bernardi, The calculation of small molecular interactions by the differences of separate total energies. Some procedures with reduced errors, Mol. Phys. 19 (1970) 553–566.
[41] (a) J.P. Foster, F. Weinhold, Natural hybrid orbitals, J. Am. Chem. Soc. 102 (1980) 7211–7218;
(b) A.E. Reed, F. Weinhold, Natural bond orbital analysis of near-Hartree–Fock water dimer, J. Chem. Phys. 78 (1983) 4066–4073;
(c) A.E. Reed, R.B. Weinstock, F. Weinhold, Natural-population analysis, J. Chem. Phys. 83 (1985) 735–746;
(d) A.E. Reed, F. Weinhold, Natural localized molecular orbitals, J. Chem. Phys. 83 (1985) 1736–1740;
(e) J.E. Carpenter, Extension of Lewis structure concepts to open-shell and excited-state molecular species, Ph.D. Thesis, University of Wisconsin, Madison, WI, 1987;
(f) J.E. Carpenter, F. Weinhold, Analysis of the geometry of the hydroxymethyl radical by the different hybrids for different spins natural bond orbital procedure, J. Mol. Struct. (Theochem.) 46 (1988) 41–62;
(g) A.E. Reed, L.A. Curtiss, F. Weinhold, Intermolecular interactions from a natural bond orbital, donor–acceptor viewpoint, Chem. Rev. 88 (1988) 899–926;
(h) F. Weinhold, J.E. Carpenter, in: R. Naaman, Z. Vager (Eds.), The Structure of Small Molecules and Ions, Plenum, 1988, pp. 227–236.
[42] B.H. Besler, K.M. Merz Jr., P.A. Kollman, Atomic charges derived from semiempirical methods, J. Comput. Chem. 11 (1990) 431–439.

[43] U.C. Singh, P.A. Kollman, An approach to computing electrostatic charges for molecules, J. Comput. Chem. 5 (1984) 129–145.
[44] P.S. Sedano, Implementation and Application of Basis Set Superposition Error-Correction Schemes to the Theoretical Modeling of Weak Intermolecular Interactions, Dissertation of Doctor in Philosophy, University of Girona, Girona, 2001.
[45] D.B. Depizzol, M.H.M. Paiva, T.O. Dos Santos, A.C. Gaudio, MoCalc: a new graphical user interface for molecular calculations, J. Comput. Chem 26 (2) (2005) 142–144.
[46] J.M. Pires, W.B. Floriano, A.C. Gaudio, Extension of the frontier reactivity indices to groups of atoms and application to quantitative structure–activity relationship studies, J. Mol. Struct. (Theochem.) 389 (1997) 159–167.
[47] S.M. Raman, V. Ponnuswamy, P. Kolandaivel, K. Perumal, Ultrasonic and DFT study of intermolecular association through hydrogen bonding in aqueous solutions of glycerol, J. Mol. Liq. 142 (2008) 10–16.
[48] H.V. Koningsveld, Symmetric αα conformation (X-ray analysis), Recl. Trav. Chem. Pays-Bas 87 (1968) 243–254.
[49] K.J. Wynne, Crystal and molecular structure of chloro(phthalocyaninato) gallium(III), Ga(Pc)Cl, and chloro(phthalocyaninato)aluminum (III), Al(Pc)Cl, Inorg. Chem. 23 (1984) 4658–4663.
[50] J. Janczak, R. Kubiak, X-ray single crystal investigations of magnesium phthalocyanine. The 4 + 1 coordination of the Mg ion and its consequence, Polyhedron 20 (2001) 2901–2909.
[51] M.T. Nguyen, A.K. Chandra, S. Sakai, K. Morokuma, Another look at the mechanism of the concerted 1,3-dipolar cycloaddition of fulminic acid to acetylene, J. Org. Chem. 64 (1999) 65–69.
[52] L.T. Nguyen, F.D. Proft, A.K. Chandra, T. Uchimaru, M.T. Nguyen, P. Geerlings, Nitrous oxide as a 1,3-dipole: a theoretical study of its cycloaddition mechanism, J. Org. Chem. 66 (2001) 6096–6103.
[53] P. López, F. Meñdez, Fukui Function as a descriptor of the imidazolium protonated cation resonance hybrid structure, Org. Lett. 6 (2004) 1781–1783.
[54] Y.-L. Lin, Y.-M. Lee, C. Lim, Differential effects of the Zn–His–Bkb vs Zn–His–[Asp/Glu] triad on Zn-core stability and reactivity, J. Am. Chem. Soc. 127 (2005) 11336–11347.
[55] J. Melin, P.W. Ayers, J.V. Ortiz, Removing electrons can increase the electron density: a computational study of negative Fukui functions, J. Phys. Chem. A 111 (2007) 10017–10019.
[56] T. Sato, K. Tokunaga, K. Tanaka, Vibronic coupling in naphthalene anion: vibronic coupling density analysis for totally symmetric vibrational modes, J. Phys. Chem. A 112 (2008) 758–767.
[57] R.E. Estrada-Salas, A.A. Valladares, Exploring the surface reactivity of 3d metal endofullerenes: a density-functional theory study, J. Phys. Chem. A 113 (2009) 10299–10305.
[58] J.L. Gázquez, F. Meñdez, The hard and soft acids and bases principle: an atoms in molecules viewpoint, J. Phys. Chem. 98 (1994) 4591–4593.